

TECHNOLOGY TRANSFER OF PLATE WAVE NDE TO ULTRASONIC ROTARY ACTUATION

Yoseph Bar-Cohen
Jet Propulsion Laboratory,
California Institute of Technology, Pasadena, CA 91109

INTRODUCTION

For many decades, plate waves have been the subject of NDE research and application. Recently, the accumulated knowledge has been technology transferred to actuation mechanisms. These waves, also known as guided waves or Lamb waves, can be formed in two distinct modes: symmetric and antisymmetric, with a fundamental as well as high order harmonic modes. The specific modes are defined by their vibration characteristics in relation to the plate geometry, e.g., the symmetric mode is associated with a symmetric motion over the plate center plane. Initially, these waves were applied for NDE of metallic structures [1]. After leaky Lamb waves were first observed in composite materials [2], the spotlight of the plate waves research activity was turned toward materials with orientation dependent properties. Many researchers have investigated solutions to the wave equations for propagation in anisotropic materials and as a result efficient approximation techniques and numerical solutions were developed. Using experimental methods, such as the leaky Lamb wave, pulsed pitch-catch and contact coupling, measurements accurately corroborated the theoretical predictions for the various plate wave modes [3]. These results led to the ability to determine the elastic properties of composite materials as well as adhesive bonded joints.

Generally, as can be seen from Figure 1, the surface particles motion in a traveling flexural plate wave mode (i.e., anti symmetric mode) are moving in an elliptical motion around their original location. When the particles move upward they also move backward in reference to the propagating wave (the wave moves right while the upward-rotating particle moves left). This backward movement can be harnessed to propel parts that are in an intimate contact with the vibrating plate. This effect has formed the basis for a new actuation mechanism also known as ultrasonic, solid state or piezoelectric motors [4]. The rotated object is called the rotor and the drive vibrating plate is called the stator.

ULTRASONIC MOTORS

The development of ultrasonic motors came at a time when there is an increasing demand for miniaturized mechanisms and they are offering a new form of actuation with potential capabilities that cannot be obtained with conventional actuators. NASA, in its efforts to reduce the size and mass of future spacecraft, is strongly interested in miniature actuators. The miniaturization of conventional electromagnetic motors is limited by manufacturing constraints and loss of efficiency. Generally, electromagnetic motors compromise speed for torque using speed reducing gears. The use of gears adds mass, volume and complexity as well as reduces the system reliability due to the increase in number of the system components. Ultrasonic motors are offering an effective alternative drive mechanism for

miniature instruments, provide high torque density at low speed, high holding torque, simple construction, quiet operation and quick response. These motors already emerged in commercial products, such as cameras, compact paper handling devices and watches. Under the Mars Lander Robotic Program, JPL is currently considering the use of these motors for the actuation of a robotic arm that will perform sample collection tasks on the surface of Mars. A study is currently underway to develop such motors for operation in space environment, i.e., operate effectively and reliably in vacuum and low temperatures down to cryogenic levels. The theoretical modeling and prototype development are conducted with MIT. Further, a technology transfer is being explored with a local small company (QMI, Costa Mesa, CA) under a Technology Cooperative Agreement.

PRINCIPAL OF OPERATION

Ultrasonic motors produce a gross mechanical motion by amplifying repeated micro-deformations that are induced by an active material (usually a piezoelectric wafer). As shown in Figure 1, the induced micro orbital-motion in the stator (at the point of contact with the rotor) is rectified by the frictional interface (rotor/stator) to produce macro-motion of the rotor. Teeth, arranged as a ring on the stator, are used to enhance the speed of the particles propelling effect. The rectification of the micro-motion at the interface is provided by pressing the rotor on top of the stator and the frictional force between the two causes the rotor to spin. This motion transfer operates as a gear and it leads to a rotation speed (up to about 500 rpm) that is much lower than the wave frequency (10-80 KHz).

To generate traveling waves, a piezoceramic wafer poled internally is a structure that consists of quarter wavelength out-of-phase zones. This poling pattern is also intended to eliminate extension in the stator and maximize bending. Two poled groups are formed on the wafer and are driven at 90° out-of-phase to produce two orthogonal disk modes. Using sinusoidal and cosinusoidal electric drive signals, these orthogonal modes are controlled to generate either forward or backward rotation.

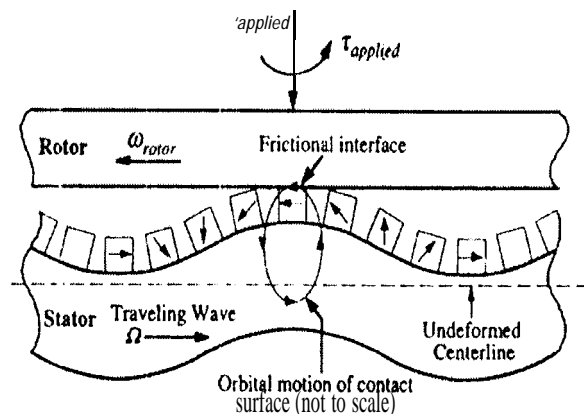


Figure 1: Principle of operation of a rotary traveling wave motor.

FUTURE DIRECTION OF THE TECHNOLOGY

The evolution of plate waves from NDE to actuation technology has offered a dual-use of the plate wave theoretical modeling base, which was initially developed for NDE. Specific concern in modeling

ultrasonic motors is the mechanical interaction at the stator rotor interface and as this issue is better handled the design of optimized motors is becoming increasingly feasible.

Currently, these motors are commercially available from Japanese manufacturers and in an experimental form from European manufacturers. All new Cannon cameras are now equipped with this motor type as the drive of the zoom lens. New applications are increasingly being reported, including CD-ROM disk drives, as well as other hardware that support the computer technology. Unfortunately, there is still no American manufacturer of ultrasonic rotary motors and the JPL effort is hoped to form such a manufacturing capability.

The stall torque (measure of the motor capability), that can be produced by commercial motors, is in the range of 0.1 to 10 in-lb. Efforts are exerted to expand this range at both ends, namely to increase the torque capability to higher levels as well as to produce actuators for micro-electromechanical systems (MEMS) [5]. MEMS is the fastest growing segment of the actuation technology and, in the coming years, it is anticipated to become a multi-billion dollar industry. "Bug"-like devices are being developed for a wide spectrum of applications that used to be considered as science-fiction. Such applications include medical micro-operation of internal organs, support search and rescue missions in earthquake and other disasters, smart structures, activation of aerospace and automotive devices and micromachining tools.

ACKNOWLEDGMENT

The research described in this publication, that was carried out by the Jet Propulsion Laboratory, California Institute of Technology, was performed under a Contract with the National Aeronautics and Space Administration and it is part of a larger task on Mars Lander Robotics (P.L., Dr. Paul Schenker, JPL.). The goal of this task is to advance mechanisms, controls and machine intelligence for next generation planetary in-situ science exploration.

REFERENCES

1. J. and H. Krautkramer, "Ultrasonic Testing of Materials", Springer-Verlag, New York (1969).
2. Y. Bar-Cohen and D. E. Chimenti, "Leaky Lamb Waves in Fiber-Reinforced Composite Plates," Review of Progress in Quantitative NDE, Vol. 3B, D. O. Thompson and D. E. Chimenti (Eds.), Plenum Press, New York (1984), pp. 1043-1049.
3. Bar-Cohen, A. K. Mal and S. -S. Lih, "NDE of Composite Materials Using Ultrasonic Oblique Insonification," Materials Evaluation, Vol. 51, No. 11, (Nov., 1993) 1285-1296.
4. W. Hagood and A. McFarland, "Modeling of a Piezoelectric Rotary Ultrasonic Motor," IEEE Transactions on Ultrasonics, Ferroelectrics and Frequency Control, Vol. 42, No. 2, 1995 pp. 210-224.
5. Flynn, et al, "Piezoelectric Micromotors for Microrobotics", J. of Microelectromechanical Systems, Vol.1, No.1, (1992) pp. 44-51.

LOW FREQUENCY GUIDED PLATE WAVE PROPAGATION IN FIBER REINFORCED COMPOSITES

Shyh-Shiuh Lih and Yoseph Bar-Cohen
Jet Propulsion Laboratory
California Institute of Technology, Pasadena, CA

Ajit K. Mal
Department of Mechanical Aerospace and Nuclear Engineering
University of California Los Angeles, CA

INTRODUCTION

The use of composite materials has increased steadily during the past two decades, particularly for aerospace, underwater and automotive structures. This is largely because many composite materials exhibit high strength-to-weight and stiffness-to-weight ratios, which make them ideally suited for use in weight-sensitive structures. The elastic properties of composite materials may be significantly different in specimens manufactured under the same general specifications and the bulk material properties may be different from those of the lamina. The elastic properties degrade as a result of aging, environmental and other effects (e.g., matrix cracking) resulting in overstress and eventual failure of the material. The elastic properties determine the performance of the material and it is necessary to assure the conformance of these properties with design requirements. Conventional destructive techniques for determining the elastic stiffness constants can be costly and often inaccurate. This is particularly true for the through-the-thickness properties. Nondestructive determination of these properties offers a better alternative for material characterization and for assuring structural performance.

A systematic analytical method proposed by Mal, Lih and Bar-Cohen [1], employing the leaky Lamb wave (LLW) phenomenon, has been found to be an effective method for the characterization of the elastic constants. The model assumes that the composite material consists of transversely isotropic layers and the transmission of the ultrasonic signals requires the use of water immersion or water injection through squirters. Dispersion curves (phase velocity vs. thickness times frequency) are measured and are used to determine the elastic constants using an inversion algorithm. The water coupling requirement restricts the field applicability of the method and limits the number of constants that can be measured. Particularly, the constant c_{11} is difficult to determine due to practical difficulties that are associated with setting up experiments with small incidence angles. The application of a contact-coupled guided-wave method offers the potential for a practical nondestructive characterization method.

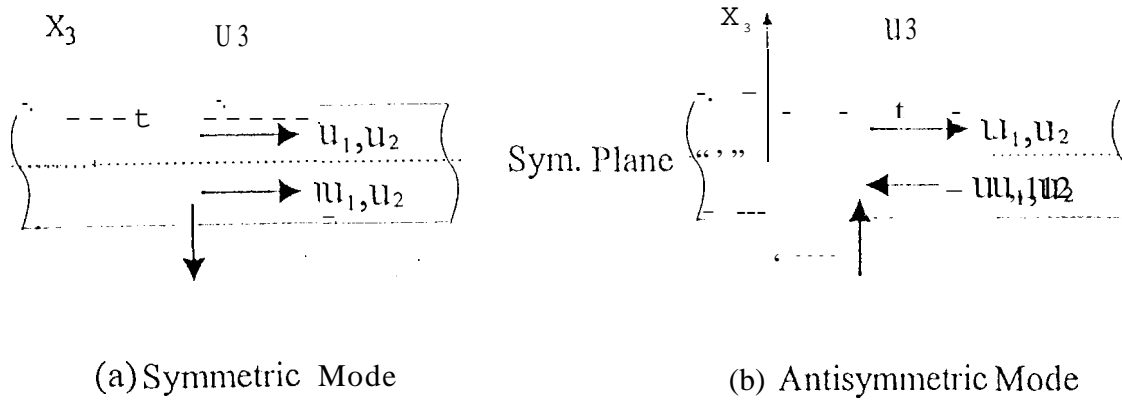


Figure 1. Definition of the geometrical variables of the symmetric and antisymmetric guided wave modes.

The theoretical and experimental studies of guided wave propagation in composites have grown considerably in recent years [2, 3]. A homogeneous composite laminate with the axis of symmetry parallel to the surfaces (Figure 1), supports the formation of two modes of propagation: symmetric and antisymmetric. The lowest symmetric (extensional) and antisymmetric (flexural) modes are the easiest to measure in an ultrasonic experiment and their velocity value can be used to determine certain material constants. German [4] has developed an ultrasonic technique which is based on a contact type transducer-pair arrangement that can be used to measure the dispersion curves of the low frequency flexural mode, and to determine the elastic properties. Unfortunately, the flexural wave signals are usually mixed with reflected signals from the boundary if the lateral dimensions of the specimen are small in relation to the wavelength or if the geometry is complex. In this case, only the extensional mode can be identified clearly.

A systematic parameter study was conducted [1] and is showing that the stiffness constants c_{11} , c_{22} , c_{23} , and c_{55} have a strong influence on the dispersion curves for the lowest symmetric extensional mode in the low frequency range. In Figure 2, the dispersion curve for the symmetric mode for wave propagation along the fibers is plotted. In this figure, the strong effect of c_{11} can be easily observed. In this study, a detailed analysis of the low frequency symmetric guided waves was conducted and the results corroborated experimentally.

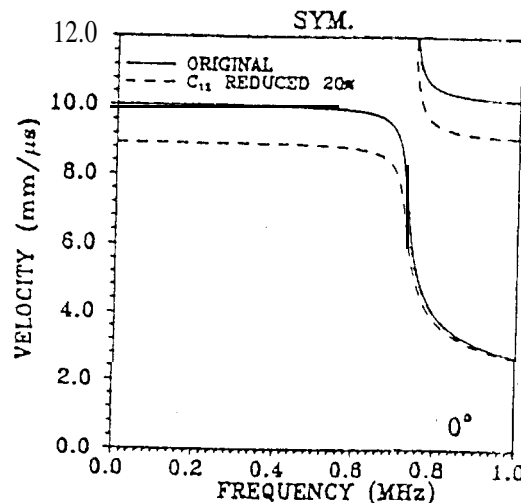


Figure 2. The influence of the elastic constant c_{11} on the dispersion curve of the symmetric mode.

FORMULATION OF SYMMETRIC MODE DISPERSION EQUATION

Exact Linear Elastic Solution

Generally, the dispersion equations for guided wave propagation in composite materials are very complicated and need to be solved numerically. The exact equations for the dispersion curves for Lamb wave propagation in multilayered composite laminates has been derived by many authors (e.g., Mal [5]). However the derived equations are highly nonlinear and the numerical solution is computationally intensive. In the low frequency range, approximations can be made to simplify the solution for the lowest extensional mode. A unidirectional composite laminate is assumed transversely isotropic with symmetric axis along the fiber direction, The symmetry axis is defined as the x_1 -axis of the coordinate system and the stress-displacement relations are given explicitly in [5], where $c_{11}, c_{12}, c_{22}, c_{23}, c_{55}$ are the five independent real stiffness constants of the material. We also introduce five constants a_1, a_2, a_3, a_4 and a_5 related to C_{ij} and the density of the material, ρ through

$$\begin{aligned} a_1 &= c_{22}/\rho, \quad a_2 = c_{11}/\rho, \quad a_3 = (c_{12} \cdot c_{55})/\rho \\ a_4 &= (c_{22} - c_{23})/2\rho, \quad a_5 = c_{55}/\rho. \end{aligned} \quad (1)$$

The dispersion equation for the symmetric mode can be expressed as [5]

$$\Delta_1 \cot(\zeta_1 \omega h) + \Delta_2 \cot(\zeta_2 \omega h) + \Delta_3 \cot(\zeta_3 \omega h) = 0 \quad (2)$$

where $h = H/2$ and H is the plate thickness. In the limit, where frequency approaches zero, i.e. $\omega h \rightarrow 0$, the dispersion equation becomes

$$\frac{\Delta_1}{\zeta_1} + \frac{\Delta_2}{\zeta_2} + \frac{\Delta_3}{\zeta_3} = 0 \quad (3)$$

which can be expanded as

$$\begin{aligned} &(\rho V^2 - c_{55} n_1^2)(\rho V^2 - c_{11} n_1^2) \Omega(c_{ij}, n_1, n_2) = 0 \\ &\Omega(c_{ij}, n_1, n_2) = (-c_{12}^2 c_{55} + c_{11} c_{22} c_{55}) n_1^4 + (-2c_{12}^2 c_{22} \\ &+ c_{11} c_{22}^2 + 2c_{12}^2 c_{23} - c_{11} c_{23}^2 - 2c_{12} c_{22} c_{55} + 2c_{12} c_{23} c_{55}) n_1^2 n_2^2 + (c_{22}^2 c_{55} - c_{23}^2 c_{55}) n_2^4 \\ &\cdot [(c_{12}^2 - c_{11} c_{22} - c_{22} c_{55}) n_1^2 + (-c_{22}^2 + c_{23}^2 - c_{22} c_{55}) n_2^2] \rho V^2 + c_{22} \rho V^4. \end{aligned} \quad (4)$$

Here the equation $\Omega(c_{ij}, n_1, n_2) = 0$ represents the dispersion equation of the limit of the lowest symmetric mode and $n_1 = \cos \phi, n_2 = \sin \phi$, and ϕ is the angle of propagation with the fibers. This equation can be simplified in special propagation directions as follows:

a. For propagation along the symmetric axis (O'), the dispersion equation becomes

$$(\rho V^2 - c_{55})(c_{22} \rho V^2 - c_{12}^2 - c_{11} c_{22}) = 0 \quad (5)$$

so that

$$v_{1,2} = \sqrt{\frac{c_{55}}{\rho}}, \quad \sqrt{\frac{c_{11} - c_{12}^2/c_{22}}{\rho}} \quad (6)$$

b. For propagation perpendicular to the symmetric axis (90°), the equation can be simplified to

$$(p V^2 - c_{55})(c_{22} \rho V^2 - c_{22}^2 + c_{23}^2) = 0 \quad (7)$$

so that

$$v_{1,2} = \sqrt{\frac{c_{55}}{\rho}}, \sqrt{\frac{c_{22} - c_{23}^2/c_{22}}{\rho}} \quad (8)$$

For an isotropic material, the solutions (6) and (8) can be reduced to the well know expression

$$V_{1,2} = \sqrt{\frac{c_{55}}{\rho}}, 2\sqrt{\frac{c_{55}}{\rho} \sqrt{1 - \frac{c_{55}}{c_{11}}}} \quad (9)$$

Approximate Plate Theories

For low frequency guided wave propagation in composite laminates, various approximate models have been proposed [8]. It is well known that classical plate theories underestimate the deflections as well as the stresses and overestimate the phase velocity of the propagating waves. The error associated with the calculation grows significantly with the increase in plate thickness or frequency; hence, for dynamic analysis of high values of thickness-times-frequency, the classical plate theories are inadequate. Mindlin and others [7] proposed an improved approximation using the first order shear deformation theory and retaining the transverse shear and rotary inertia of the plate elements. Based on this theoretical approach the dispersion curves of the first *antisymmetric mode* can be approximated very closely to the exact solutions [8]. According to this theory, the displacement components are assumed to be of the form

$$\begin{aligned} u_1 &= u_1^0(x_1, x_2, t) + x_3 \psi_1(x_1, x_2, t) \\ u_2 &= u_2^0(x_1, x_2, t) + x_3 \psi_2(x_1, x_2, t) \\ u_3 &= u_3^0(x_1, X_2, t) \end{aligned} \quad (10)$$

where u_1^0, u_2^0 and u_3^0 are the displacement components of a point in the mid-plane, and ψ_1 and ψ_2 are the rotations of a line element, originally perpendicular to the longitudinal plane about the x_2 and x_1 axes, respectively. However, based on this assumption, the lowest symmetric modes are nondispersive as in the classical plate theory. This is the result of ignoring the fact that u_1 and u_2 are even functions of x_3 , and u_3 is an odd function of x_3 for the symmetric mode (Figure 1a). In order to obtain a high order approximate symmetric mode dispersion curve, a term $x_3 \psi_3$ is included in the out-of-plane displacement u_3 .

$$\begin{aligned} u_1 &= u_1^0(x_1, X_2, t) \\ u_2 &= u_2^0(x_1, X_2, t) \\ u_3 &= x_3 \psi_3(x_1, x_2, t) \end{aligned} \quad (11)$$

Hence, the governing equation for the symmetric mode can be written as

$$\begin{pmatrix} A_{11}\frac{\partial^2}{\partial x_1^2} + A_{55}\frac{\partial^2}{\partial x_2^2} & (A_{12} + A_{55})\frac{\partial^2}{\partial x_1\partial x_2} & A_{12}\frac{\partial}{\partial x_1} \\ (A_{12} + A_{55})\frac{\partial^2}{\partial x_1\partial x_2} & A_{55}\frac{\partial^2}{\partial x_1^2} + A_{22}\frac{\partial^2}{\partial x_2^2} & A_{23}\frac{\partial}{\partial x_2} \\ A_{12}\frac{\partial}{\partial x_1} & A_{23}\frac{\partial}{\partial x_2} & D_{55}\frac{\partial^2}{\partial x_1^2} + D_{44}\frac{\partial^2}{\partial x_2^2} + A_2 \end{pmatrix} \begin{pmatrix} u_1 \\ u_2 \\ \Psi_3 \end{pmatrix} = \begin{pmatrix} I_1 \ddot{u}_1 \\ I_2 \ddot{u}_2 \\ I_3 \ddot{\Psi}_3 \end{pmatrix} \quad (12)$$

The dispersion equation can be derived from the following eigenvalue equation:

$$\begin{vmatrix} -(A_{11}k_1^2 + A_{55}k_2^2) + I_1\omega^2 & -(A_{12} + A_{55})k_1k_2 & iA_{12}k_1 \\ -(A_{12} + A_{55})k_1k_2 & -(A_{55}k_1^2 + A_{22}k_2^2) + I_1\omega^2 & iA_{23}k_2 \\ iA_{12}k_1 & iA_{23}k_2 & D_{55}k_1^2 + D_{44}k_2^2 + A_{22} + I_3\omega^2 \end{vmatrix} = 0 \quad (13)$$

where $k_1 = \omega/V n_1$, $k_2 = \omega/V n_2$ and V is the phase velocity. A_{ij} , B_{ij} and D_{ij} are the commonly used generalized elastic parameters for composite laminates.

$$\begin{aligned} A_{11} &= c_{11}H, A_{12} = c_{12}H, A_{22} = c_{22}H, A_{55} = c_{55}H, A_{23} = c_{23}H \\ D_{55} &= c_{55}I_3/\rho, D_{44} = c_{44}I_3/\rho, c_{44} = (c_{22} - c_{23})/2 \\ I_1 &= \rho H, I_3 = \rho H^3/12 \end{aligned} \quad (14)$$

If the laminate is a transversely isotropic material, then the approximate dispersion equation can be expressed as

$$\begin{aligned} &(-c_{12}^2 c_{55} - c_{11} c_{22} c_{55})n_1^4 + (-2c_{12}^2 c_{22} - c_{11}^2 c_{22} - 2\hat{c}_{12} \hat{c}_{23} - c_{11} c_{23}^2 \\ &- 2c_{12} c_{22} c_{55} + 2c_{12} c_{23} c_{55})n_1^2 n_2^2 + (c_{22}^2 c_{55} - c_{23}^2 c_{55})n_2^4 \\ &+ [(c_{12}^2 - c_{11} c_{22} - c_{22} c_{55})n_1^2 + (-c_{22}^2 - c_{23}^2 - c_{22} c_{55})n_2^2] \rho V^2 + c_{22} \rho V^4 + O((\omega H)^2) = 0 \end{aligned} \quad (15)$$

In the limit $\omega H \rightarrow 0$ this equation is the same as equations (4). Note that high order approximations such as

$$\begin{aligned} u_1 &= u_1^0(x_1, x_2, t) + x_3^2 \eta_1(x_1, x_2, t), \\ u_2 &= u_2^0(x_1, x_2, t) + x_3^2 I_2(x_1, x_2, t), u_3 = x_3 \Psi_3(x_1, x_2, t) \end{aligned} \quad (16)$$

can lead to more accurate results but they will increase the complexity of the dispersion equation.

Furthermore, depending on the experimental setup, the measured wave velocity can be either the phase or the group velocity. The group velocity V_g can be calculated from the characteristic equation of the phase velocity by

$$V_g = - \frac{\partial \Omega / \partial n}{\partial \Omega / \partial V} \quad (17)$$

EXPERIMENTAL APPROACH

An experimental setup was designed to determine low frequency measurements of the dispersion curves. The setup consisted of a contact pitch-catch arrangement, where the pulse source was induced by breaking a pencil lead on the surface of the test sample. Three identical receiving transducers were placed in contact with the composite laminate along one line that defined the angle of propagation and they were spaced at a distance of 25 mm apart. The transducers were a broadband type with 5 MHz center frequency (Digital Waves, Model 1]1000). For data acquisition a Fracture Wave Detector (Digital Waves, F4000) with four signal conditioning modules was used. Each of the transducers was connected to a wideband preamplifier through a signal conditioning module and the signals were digitized and recorded at a rate of 3.125 MHz to 25 MHz. A schematic view of the experimental setup is shown in Figure 3. A $[0]_{16}$, 12 x 12 cm² unidirectional AS4/3502 (1 Hercules) graphite/epoxy laminate was used as the test sample. The laminate was produced using a standard hot-press curing technique, which led to a laminate thickness of 3.175 mm. The emphasis of the current study was on the inversion of fiber dominated properties c_{11} and c_{12} . For this purpose material density of $\rho = 1.56 \text{ g/cm}^3$ was used and the matrix dominated material constants, c_{22} , c_{23} , and c_{55} , were predetermined using leaky Lamb waves and the inversion technique described in [1] as follows: $c_{22} = 15.6$, $c_{23} = 7.89$, $c_{55} = 5.00$ (GPa).

The use of the pencil-lead breaking method as the source of signals was chosen since the signals that are produced have a low frequency broadband spectra in the range of 50 to 100 KHz. The data for each received signal was transferred to a personal computer and processed to determine the wave velocity for the analysis of the dispersion curve. Measurements were made along different directions with the fibers at 1° intervals from 0° to 90° and the three receivers were placed at a distance 25 mm, 50 mm and 75 mm from the source. For various directions of the transducers placement, the group velocity was determined from the time-of-flight measurements using the arrival of the first received signal.

RESULTS AND CONCLUDING REMARKS

Dispersion curves for the exact and approximate solution of the symmetric mode are plotted in Figure 4. This figure shows the phase velocity of a unidirectional graphite/epoxy at 45° to the fibers. It can be seen that the approximate solution agrees with the exact solutions for the frequency times thickness values lower than 0,7 MI Iz-mm. Further, this approximation allows the calculation of modes that can not be obtained using the classical plate theory.

The measured and calculated group velocity for wave propagation at the 0° to 90° with the fibers are presented in Figure 5. The elastic constants c_{11} , c_{12} were determined by inversion of the measured group velocity and they are: $c_{11} = 155.01$, $c_{12} = 6.44$ (GPa). It can be seen that the calculated curves fit the experimental data quite well. However, it is known that the group velocity of the extensional mode in this frequency range may not be sensitive to some of the elastic constants. In order to characterize the material constants from the measured group velocity, a parametric study was carried out and is presented in Figure 6. In the figure the group velocity curve is plotted for the lowest symmetry mode. From this figure, one can easily see that c_{11} has the strongest influence on the group velocity curve near 0° and decreases toward zero at about 45°.

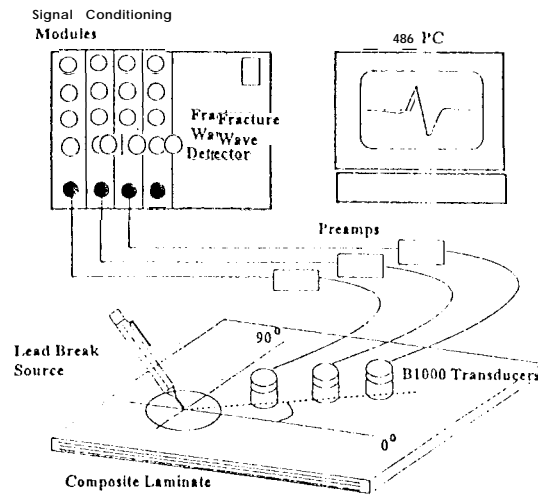


Figure 3. A schematic description of the experimental setup.

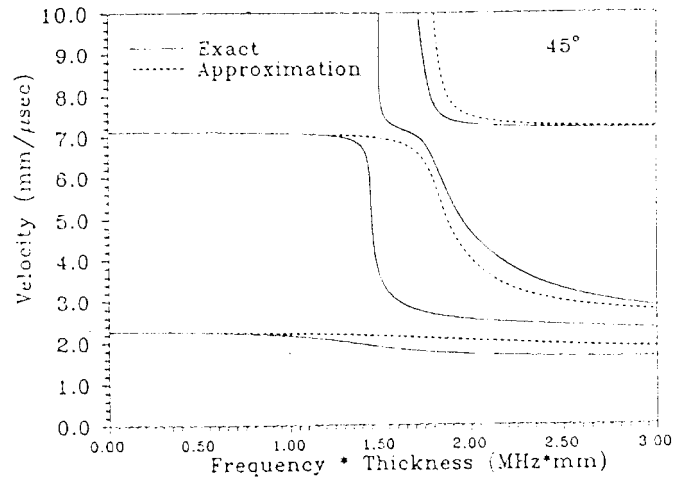


Figure 4. Comparison of dispersion curves for a 1 mm thick graphite/epoxy plate between exact theory and shear deformation theory for wave propagation at 45° to fibers.

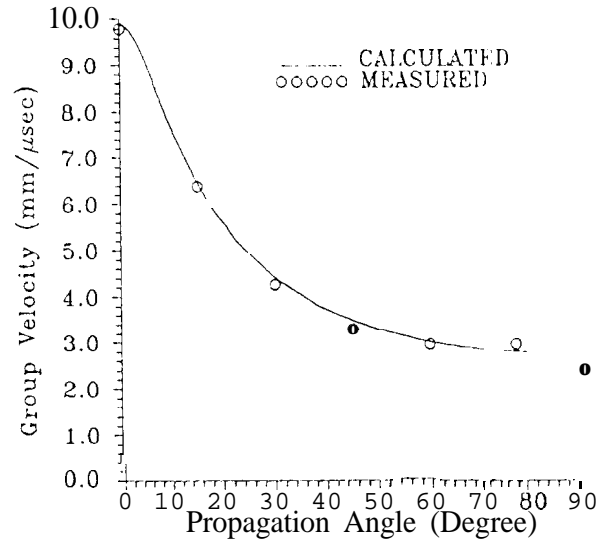


Figure 5, Measured and calculated group velocities for the extensional wave mode s_0 propagating at 0° to 90° with the fibers in a unidirectional graphite/epoxy plate of 3.175 mm thickness.

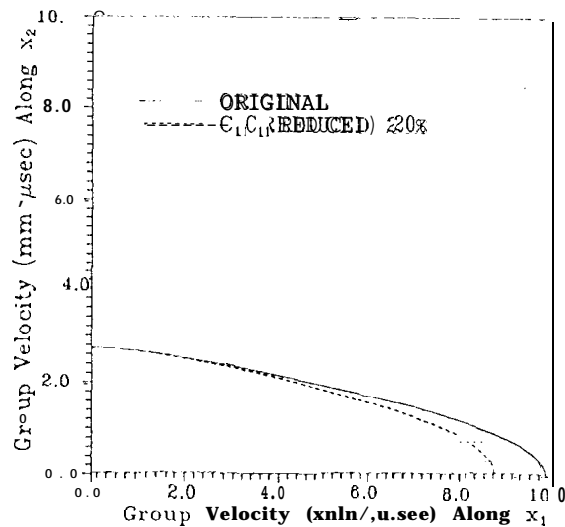


Figure 6. Influence of the stiffness constant c_{11} on the group velocity surface for the lowest symmetric mode of a unidirectional graphite/epoxy laminate.

ACKNOWLEDGMENT

This research was supported by the AFOSR under grant F49620-93-1-0320 monitored by Dr. Walter Jones. The JPL portion of the research was carried out under a contract with NASA.

REFERENCES

1. A. K. Mal, S. Lih and Y. Bar-Cohen, Proceedings of the ASME/ASCE/AHS/ASC Structures, Structural Dynamics and Materials Conference, Part 1, A-93-1349-CP, La Jolla, CA, (April 19-22, 1993) pp. 472-484.
2. A.K. Mal and Y. Bat-Cohen, *ASME-SES Symposium on Wave Propagation in Structural Composites*, A.K. Mal and T.C.T Ting (Eds.) ASME-AMD-Vol. 90, (1988) pp. 1-16.
3. S.K. Datta and T. Shah, Charkraborty and R. I. Bratton, *ASME-SES Symposium on Wave Propagation in Structural Composites*, A.K. Mal and T.C.T Ting (Eds.) ASME-AMD-Vol. 90, (1988), pp. 1-16.
4. M. Gornan, *J. Acoust. Soc. Am.* Vol. 90, No. 1, (1991), pp. 358-364.
5. A. K. Mal, "Wave Propagation in Layered Composite Laminates Under Periodic Surface Loads", *Wave Motion*, Vol. 10, (1988), pp. 257-266.
6. F.C. Moon, *J. Comp. Mater.*, Vol. 6, (1972), pp. 62.
7. R.D. Mindlin, "Waves and Vibration in Isotropic, Elastic Plates", *Structural Mechanics*, (1960), pp. 199-232
8. S. Lih and A. K. Mal, "On the Accuracy of Approximate Plate Theories for Wave Field Calculations in Composite Laminates", *Wave Motion*, Vol. 21, (1995), pp. 17-34.